MOLEKUL
eISSN: 2503-0310

Articles
https://doi.org/10.20884/1.jm.2025.20.2.14891

# Harnessing Nature's Colors: Combining Plant Pigments and Metal Coatings for Dye-Sensitized Solar Cell

Hardeli[1], Hary Sanjaya[1], Lasmi Yunita[1], Indri Panca Novita[1], Nurul Fadilah Agdisti[1], Rahmaneta Luli[1], Putri Permatasari[2]*

[1]Department of Chemistry, Universitas Negeri Padang, Padang 25131, Indonesia
[2]Department of Materials Science and Processing, Gifu University, Gifu 501-1113, Japan

*Corresponding author email: putri.permatasari.s4@s.gifu-u.ac.jp

**Received** February 07, 2025; **Accepted** May 08, 2025; **Available online** July 20, 2025

**ABSTRACT.** This study aims to improve the efficiency of dye-sensitized solar cells (DSSCs). To overcome the recombination problem in the commonly used $TiO_2$ semiconductor, we performed electrodeposition of ferrous metal (Fe) on $TiO_2$. XRD characterization showed that after Fe electrodeposition, the crystal structure of $TiO_2$ remained in the anatase phase without significant changes compared to before deposition while based on SEM-EDS results, Fe was dispersed to form small agglomerates that functioned as metal contacts to reduce electron recombination. We also investigated the use of anthocyanins from various natural sources, including jengkol skin, senduduk fruit, mangosteen skin, and red grape skin. These anthocyanins were copigmented with salicylic acid. UV-Vis spectroscopy revealed that copigmentation caused a bathochromic shift and FTIR spectrum confirmed strong interaction between anthocyanins and salicylic acid through hydrogen bond formation. The combination of $TiO_2$-Fe layers with pigmented dyes resulted in diverse DSSC efficiencies, with mangosteen peel showing the best performance (4.123%), followed by senduduk fruit (3.495%), grape peel (2.569%), and jengkol peel (1.925%). The increase in efficiency from 1.189% (without Fe coating) to 1.700% (with Fe coating) demonstrates the potential of this technique. The small $TiO_2$ crystal size (about 61.8 nm) also contributes to the increased surface area, enhancing dye absorption and solar cell performance. The electrical efficiency showed that the combination of $TiO_2$-Fe with copigmented anthocyanins from mangosteen skin produced DSSCs with the highest efficiency, demonstrating the potential of this approach to improve the performance of natural dye-based solar cells.

**Keywords**: Co-pigmentation, dye-sensitized solar cell, Fe electroplating, natural dye.

## INTRODUCTION

Energy is one of the biggest challenges we face in this modern era (Sofian et al., 2024; Gorinanet al., 2024; Jiglau et al., 2024; LaBelle, 2023; Pashiri et al., 2022). Along with rapid economic and population growth, energy demand continues to rise sharply (Ahmed et al., 2023; Mombekova et al., 2024; Wang et al., 2023). While fossil fuels still dominate the main energy sources, we are on the verge of a major shift towards the era of renewable energy (Nijsse et al., 2023; Sahin et al., 2024). Amidst various renewable energy options such as wind, hydro, and biomass, solar energy is emerging as a very promising candidate, especially in a tropical country like Indonesia (Pambudi et al., 2023; Silalahi et al., 2021). Indonesia's geographical location on the equator provides the advantage of abundant sun exposure throughout the year, making it an ideal location for the development of solar cell technology (Bernabé-Poveda et al., 2024; Pollin, 2023; Wuryanti & Megawati, 2019).

One exciting innovation in solar cell technology is the Dye-Sensitized Solar Cell (DSSC) (Badawy et al., 2024; Badawy et al., 2022; Dragonetti & Colombo, 2021; Muñoz-García et al., 2021; Rahman et al., 2023). DSSCs offer a unique and efficient approach in converting solar energy into electricity. Unlike conventional silicon solar cells, DSSCs use organic dyes to absorb light (Badawy et al., 2024; Barichello et al., 2024; D'Amico et al., 2023; Zdyb & Krawczak, 2021). The advantages of DSSCs lie in their flexibility and relatively low production costs (Badawy et al., 2024; Mariotti et al., 2020). The cell does not require high-purity materials, making the production process simpler and more economical (Hardeli et al., 2023; Kusuma, 2017). The working principle of DSSCs is also interesting: dye molecules absorb photons, while nanocrystalline inorganic semiconductors play a role in charge separation (Badawy et al., 2024; Darmawan & Nuzuluddin, 2023; Rahman et al., 2023; Sharma et al., 2018a; Widiatmoko et al., 2024). This approach differs from silicon-based solar cells, where silicon plays a dual role in light absorption and charge separation (Lee et al., 2014).

Titanium dioxide ($TiO_2$) is often the first choice as a semiconductor in DSSCs. Its nature as an n-type semiconductor with a relatively wide band gap (around 3.2 eV) makes it ideal for this application (Abdullah et al., 2017; Benesperi et al., 2018; Longo & De Paoli, 2003; Sharma et al., 2018b). The lower conduction band position of $TiO_2$ from the LUMO (Lowest Unoccupied Molecular Orbital) level of the dye facilitates efficient electron transfer (Badawy et al., 2024; Elmorsy et al., 2023; Leela Devi, De, Kuchhal, & Pachauri, 2024; Mustafa et al., 2023). In addition, $TiO_2$ also excels in terms of price and minimal environmental impact (Chauke et al., 2024; Gatou et al., 2024; R. Li et al., 2020; Racovita, 2022; Rodríguez-Rojas et al., 2024). However, the use of $TiO_2$ also faces challenges, especially the problem of electron recombination (Bonomo et al., 2020). This phenomenon occurs when free electrons release energy and return to the valence band, reducing cell efficiency (Leijtens et al., 2016; Sherkar et al., 2017).

To address this, metal electrodeposition techniques on $TiO_2$ layers are emerging as a promising solution. In this study, we explored the use of ferrous metal (Fe) to improve the performance of DSSCs. The selection of Fe was based on several considerations. Fe's electron configuration like that of ruthenium and osmium - metals that have been shown to yield high efficiencies in dye solar cells - was the main reason (Chen et al., 2024; Nyamukamba et al., 2018; Rahman et al., 2023; Thu et al., 2016). In addition, Fe has advantages in terms of abundance, ease of access, and lower cost (Baruah et al., 2024; Emerson et al., 2024). Fe's characteristics of being soluble in polar solvents and having a UV-Vis wavelength of 551 nm also favor its use in DSSCs (Bella et al., 2015; Mauri et al., 2022; Setyawati et al., 2017; Tuharin et al., 2020).

Another key aspect in DSSC optimization is dye selection (Arjmand et al., 2022; Badawy et al., 2024; Azra et al., 2024; Rahman et al., 2023; Triyanto et al., 2024). Although $TiO_2$ can only absorb 5% of the solar light spectrum in the UV range, the use of appropriate dyes can significantly increase the light absorption efficiency (Augustowski et al., 2021; Chauke et al., 2024; Elmorsy et al., 2023; Gnida et al., 2021; Hsu et al., 2024). In this context, natural dyes offer several advantages, including abundant availability, low cost, and simple extraction process (Li et al., 2022; Novita et al., 2024; Salauddin et al., 2021). Anthocyanins, as one of the natural dyes, have attracted the attention of researchers to be developed as sensitizers in DSSCs (Hardeli et al., 2022; Mulijani et al., 2020; Setyawati et al., 2017). Its ability to expand the light absorption area has the potential to increase cell efficiency. The presence of carbonyl and hydroxyl groups in the anthocyanin molecular structure facilitates good attachment to the $TiO_2$ layer, which in turn increases the energy conversion efficiency (Calogero et al., 2012; Dai & Rabani, 2002; Maurya et al., 2016; Prabavathy et al., 2017; Subramanian & Wang, 2012). In this study, we explored the use of anthocyanins from various natural sources, including *jengkol* (*Pithecellobium jiringa B.*) skin, *senduduk* (*Melastoma malabathricum L.*) fruit, mangosteen (*Garcinia mangostana L.*) skin, and red grape (*Vitis vinifera*) skin. However, given the easily oxidized and degraded nature of anthocyanins, we applied a co-pigmentation technique with salicylic acid to improve their stability (Zhu et al., 2020).

The main objective of this study is to evaluate the effect of Fe electrodeposition on the performance of $TiO_2$-based DSSCs, using co-pigmented anthocyanins from various natural sources as colorants. Through this approach, we hope to make significant contributions in the development of more efficient and sustainable DSSCs, opening new avenues in the utilization of solar energy in the future.

## EXPERIMENTAL SECTION

### Materials

Red grape peel (*Vitis vinifera*), mangosteen peel (*Garcinia mangostana L.*), *senduduk* fruit (*Melastoma malabathricum L.*), and *jengkol* peel (*Pithecellobium jiringa B.*) were among the natural materials that were used as samples. $Fe(NO_3)_3{\cdot}9H_2O$ (≥99%, Sigma-Aldrich), $TiO_2$ Degussa P-25 (≥99%, Evonik), distilled water, ethanol (≥99.8%, Merck), salicylic acid (≥99%, Sigma-Aldrich), hydrochloric acid (HCl, 37%, Merck), KCl (≥99.5%, Sigma-Aldrich), KI (≥99%, Sigma-Aldrich), $I_2$ (≥99.8%, Sigma-Aldrich), polyethylene glycol (PEG, MW 6000, Sigma-Aldrich), Whatman filter paper No.42, and indium tin oxide (ITO) glasses (8–12 Ω/sq, Sigma-Aldrich) were among the materials used. ITO (Indium Tin Oxide) glass is a transparent glass coated with indium-tin oxide, which is electrically conductive and transparent to visible light, so it is widely used as an electrode in DSSC.

### Preparation of ITO Glass and $TiO_2$ Layer

After getting cut to 1.25 x 1.25 cm, ITO glass was cleaned with an ultrasonic cleaner and immersed in 70% alcohol for 60 minutes. The purpose was to get rid of anything that would interfere with the ITO glass coating process. 0.5 grams of polyvinyl alcohol (PVA) were dissolved in 50 milliliters of distilled water. To make a suspension, the mixture was heated to 80 °C on a hot plate while being agitated. 0.5 grams of powdered $TiO_2$ were added to the solution. To create a fine paste for the coating procedure, the mixture was then crushed using a mortar and pestle. The doctor blade procedure was then used to smooth the $TiO_2$ paste. After that, the glass was heated for half an hour on a hot plate to remove the water content of $TiO_2$.

### Fe Metal Electroplating

A carbon electrode and a $TiO_2$ electrode are used in the procedure. A 0.2 M electrolyte of $Fe(NO_3)_3$ was utilized. Following the electroplating procedure, the $TiO_2$ layer containing Fe was dried for 30 minutes at 100 degrees Celsius on a hot plate. The titanium used was $TiO_2$ Degussa P-25, which has a nanoparticle size and has two phases, 80% anatase, and 20% rutile. In the prepared DSSC, titanium dioxide was coated on the ITO glass using the Doctor Blade method. Titanium dioxide was coated on the ITO substrate in a paste form using polyvinyl alcohol and water. The $TiO_2$ layer was then heated to 100°C to form a $TiO_2$ layer that is firmly attached to the ITO glass. Electrodeposition was carried out in the prepared $TiO_2$ layer using $Fe(NO_3)_3$ as an electrolyte solution and Fe metal as an electrode with 9V for 20 seconds. The reactions that occur at the anode and cathode can be seen in **Figure 1**. The layer deposited with Fe metal was dried in an oven at 70°C for 10 minutes, then put in a desiccator. Heating at a low temperature was done to prevent damage to the layer that has been deposited with Fe metal.

### Thin Film Characterization on Glass Surface

X-ray diffraction (XRD) was used to determine the crystal structure of both Fe-$TiO_2$ and $TiO_2$ powder by comparing their peaks. The physical form of the active layer and the presence of Fe metal on the $TiO_2$ layer were both examined with Scanning Electron Microscopy (SEM). Characterization was carried out at a compression of 10 pa and a voltage of 20 kV.

### Preparation of Dye

50 milliliters of 96% ethanol and 10 milliliters of 1M HCl were used to extract 100 grams of each of the peels from *jengkol*, *senduduk* fruit, mangosteen, and red wine. The extraction procedure was conducted in a dark environment. To separate the residue, the extraction was filtered using Whatman filter paper No. 42 after a 24-hour period. The solvent was then extracted from the filtrate using a rotary evaporator. The extract was kept in opaque. To check if anthocyanins were still present, the residue was heated to 100°C for five minutes while 2M HCl was added. The results were said to be good when a crimson color appeared. Anthocyanin extraction methods are generally carried out using polar solvents such as ethanol, methanol, or dilute acids to increase the solubility and stability of the pigment (Zhu et al., 2020; Salauddin et al., 2021). Previous studies have shown that the use of acidic solvents can help maintain the anthocyanin structure and increase extraction efficiency (Calogero et al., 2012).

### Dyes Characterization

The absorbance of the dye that had been co-pigmented with salicylic acid was measured using the Ultraviolet-Visible (UV-Vis) Spectroscopy. Additionally, the impacts of the dye co-pigmentation procedure were also identified. The Agilent 8435 UV-Vis spectrophotometer was used to assess. The light's wavelength ranges from 400 to 800 nm. The purpose of the PerkinElmer FTIR was to identify the kinds of bonds and functional groups present in the anthocyanins that were extracted. An analysis was carried out by examining a certain spectrum or peak that denoted a specific functional group.

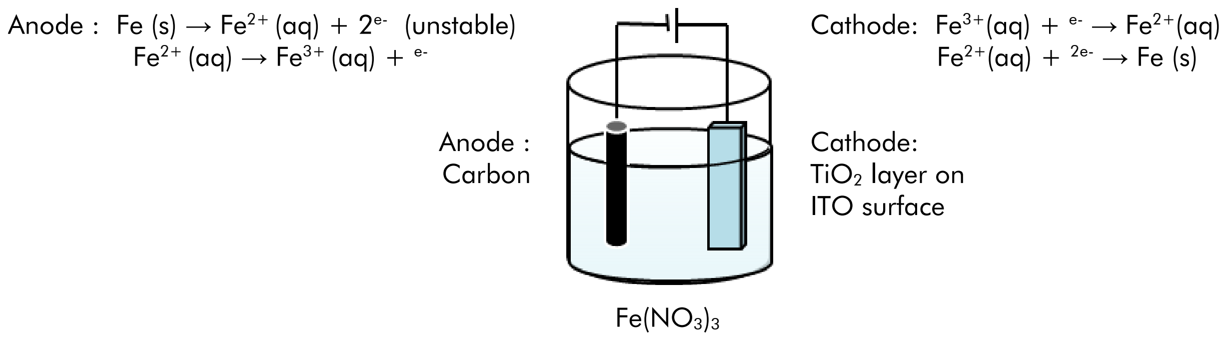


**Figure 1**. Schematic of the electrodeposition of Fe on $TiO_2$

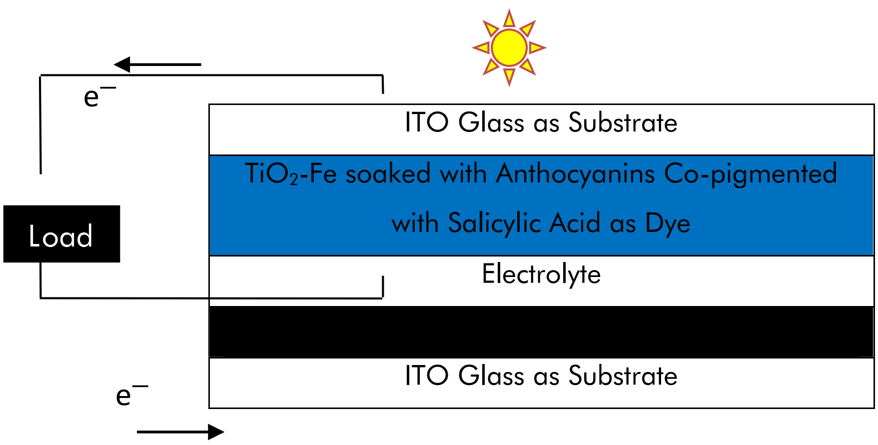


**Figure 2.** Structure of the dye-sensitized solar cells (DSSC) with $TiO_2$-Fe and natural dye co-pigmented with salicylic acid.

### Preparation of Semi-Solid Electrolyte

First, 6 mL of acetonitrile was used to dissolve 0.498 g of KI. Separately, 6 mL of acetonitrile and 0.076 g of $I_2$ were combined and stirred until the mixture was uniform. The electrolyte solution was then created by combining these two solutions. 2.4 g of PEG was then added, and the mixture was stirred until a gel was formed.

### Preparation of Counter Electrode

The carbon source for the counter electrode was graphite. It was applied on ITO glass by heating the conductive surface with a candle. After 30 minutes of heating at 450°C, the coated glass was progressively cooled to 70°C and allowed to cool down to room temperature.

### Solar Cell Fabrication

Following the creation of the DSSC's component parts, the solar cells were assembled. The sandwich-like structure of the DSSC components was put together in the sequence seen in **Figure 2**. The bottom layer is ITO glass substrate that has been coated with graphite as an electrode counter. then the electrolyte is the next layer. after that the $TiO_2$-Fe layer that has been soaked with Anthocyanins Co-pigmented with Salicylic Acid is coated on the surface using the doctor blade method which is then covered with ITO glass again as the outermost layer.

### Solar Cell Electric Current Testing

Solar cell voltage and current was monitored using an automated multimeter. UV rays were used as a light source. Because it is feared that varied light intensities will be produced if tested directly under the sun, influencing computing efficiency, light sources from ultraviolet lamps are used to get an exact and consistent source. The DSSC's photovoltaic performance was assessed by measuring current-voltage (I-V) under a simulated solar light source (AM 1.5G, 100 mW/cm$^2$). A digital source meter was used to measure electrical current and voltage while altering the external load resistance. The short-circuit current (Isc) and open-circuit voltage (Voc) were calculated directly from the I-V curve. The photocurrent generation was examined using the conventional diode (equation 1). $I_0$ represents the reverse saturation current, q the electron charge, V the applied voltage, k the Boltzmann constant, and T the absolute temperature. Equations 2 and 3 were used to obtain the fill factor (FF) and total power conversion efficiency (η). where Vmp and Imp are the voltage and current at the maximum power point, respectively, and Pin represents the incident light power.

$$I = I_0\left(e^{\frac{qV}{kT}} - 1\right) \quad (1)$$

$$FF = \frac{V_{mp}I_{mp}}{V_{oc}I_{sc}} \quad (2)$$

$$\eta = \frac{P_{out}}{P_{in}} = \frac{V_{oc}I_{sc}FF}{P_{in}} \times 100\% \quad (3)$$

## RESULTS AND DISCUSSION

### Dye Characterization

Dye-sensitized solar cells (DSSCs) use dyes to enhance their ability to absorb sunlight. The ideal dye should be able to absorb visible light strongly, stick to the semiconductor surface, and have high stability when oxidized. Anthocyanins are one of the natural dyes that can potentially be used in DSSCs. However, anthocyanins have the disadvantage of being easily damaged and oxidized. To overcome this problem, a co-pigmentation method, which combines anthocyanins with other molecules such as salicylic acid to improve their quality can be used. Through the co-pigmentation process, anthocyanins can experience significant improvements in terms of thermal stability, light-absorbing ability and durability. This process shifts the light absorption to longer wavelengths, thereby increasing the efficiency of the solar cell. In this study, we used various natural dye sources such as *jengkol* skin, *senduduk* fruit, mangosteen skin, and red grape skin. Characterization of the dyes was done using two main instruments: UV-Vis spectrophotometer to analyze the optical properties and FTIR to identify the functional groups present in the dyes. **Figure 3** shows that co-pigmentation successfully enhances the performance of anthocyanins as photosensitizers in dye-sensitized solar cells.

It was discovered that the dye spectrum produced by the four samples was almost the same. The infrared interpretation revealed the presence of the alcohol (—OH) group, as indicated by a sharp absorption at 3341.11cm$^{-1}$. Anthocyanins are compounds with a conjugated phi system that can absorb visible light. An alkene bond (C=C) was demonstrated at 1626.11cm$^{-1}$, supported by an aromatic C-H bond at 779.19 cm$^{-1}$ and an aromatic ether bond at 1247.82 cm$^{-1}$, both of which indicated the presence of a flavilum group in anthocyanidins. Furthermore, the presence of C—O—C bonds suggests the formation of bonds between anthocyanidins and sugar groups, supported by C—H bonds from the 1440.35 cm$^{-1}$ methyl group, which indicates the formation of a bond on R1 or R2 of anthocyanins. Based on the results of FTIR identification, it can be concluded that there were anthocyanin compounds in the *jengkol* skin, *senduduk* fruit, mangosteen peel, and grape skin dye extract. Therefore, it can be used as dyes in DSSC.

The UV-Vis spectrophotometer test aims to observe the effect of salicylic acid copigmentation in the dye extract. The interaction between copigment and dye is an intermolecular interaction. Salicylic acid copigmentation will produce anthocyanins with better thermal stability and the bathochromic effect, where there is a shift in maximum absorbance. The UV-Vis test results show that the dye extracts from different sources have different maximum wavelengths (λmax.).

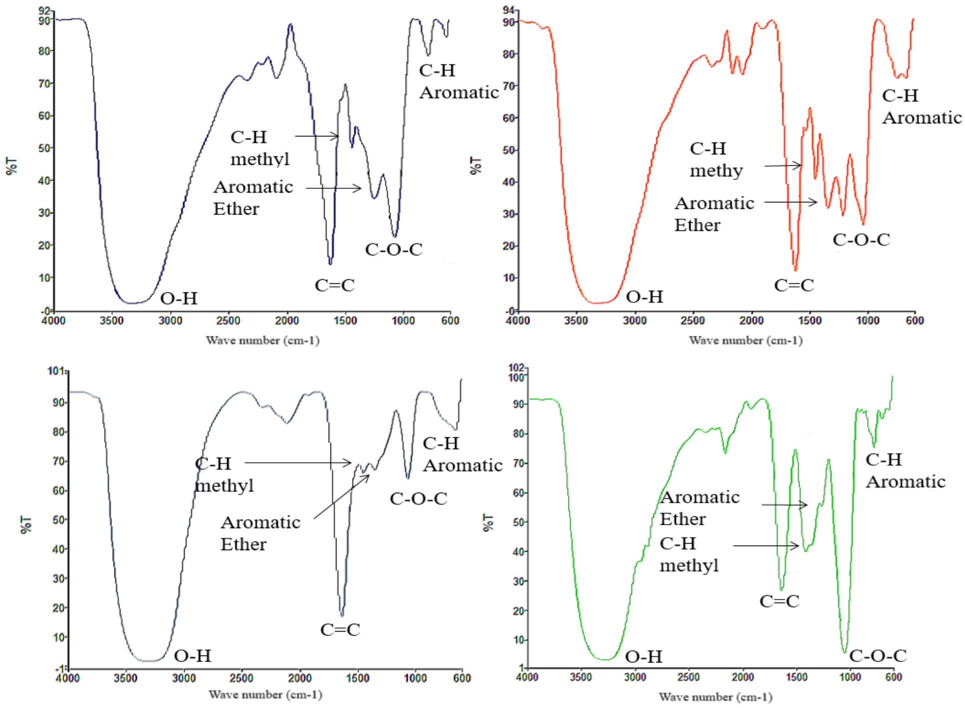


**Figure 3.** Spectra FTIR interpretation of various salicylic acid pigmented dyes: mangosteen peel (blue), jengkol skin (orange), senduduk fruit (black), and grape skin (green).

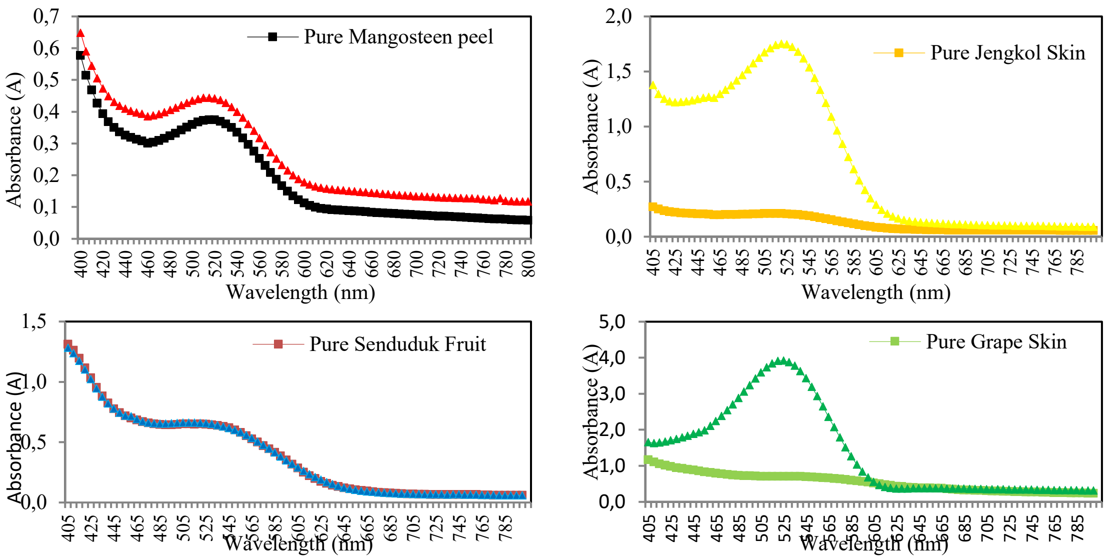


**Figure** 4. The absorbance of various salicylic acid pigmented dyes: mangosteen peel, *jengkol* skin, *senduduk* fruit, and grape skin

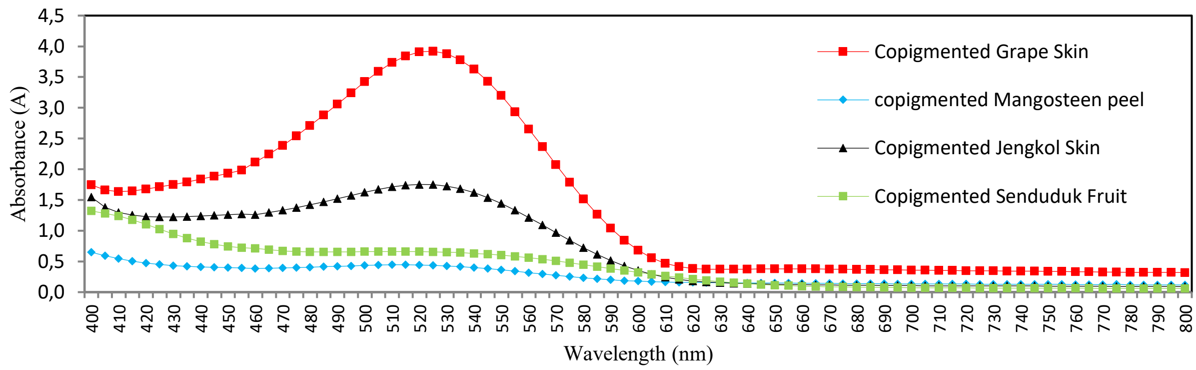


**Figure** 5. Comparison of the results of co-pigmentation of anthocyanins from various natural sources

For *jengkol* skin, the absorbance is shifted from a maximum wavelength of 515 nm without copigmentation to 520 nm for the copigmented dye. *Senduduk* fruit shifts from 505 nm to 510 nm, mangosteen shifts to 515 nm with increased intensity, and grape skin shifts from 525 nm to 535 nm. This increase happens because salicylic acid adds $\pi$ electrons to anthocyanins so that light absorption will shift to longer wavelengths. Copigments will increase the coordination between anthocyanins and others, resulting in interactions. The absorption of light at longer wavelengths can increase the absorption of sunlight by DSSC. The complex formation between copigments and anthocyanins also affects the absorption of dyes. Based on the data, copigmentation shows an increase in absorption intensity at longer wavelengths, thereby increasing light absorption and enhancing the positive effect on DSSCs.

**Fe-$TiO_2$ Layer**

ITO glass is a transparent conductive glass (TCO). It will serve as both a framework and a layer through which electrons can flow. The counter electrode used was black carbon. As a cell photocatalyst, titanium dioxide was utilized as a semiconducting layer. Heating the $TiO_2$ layer used in the Doctor Blade method at a low temperature can prevent damage to the heat-sensitive ITO glass so that the resistance of the cell can be reduced.

In the electrodeposition process, the Fe electrode acts as the anode. The electrochemical reaction that occurs at the anode was the oxidation of Fe metal to $Fe^{2+}$ ions, but $Fe^{2+}$ ions were less stable, and $Fe^{3+}$ ions were formed. At the cathode, precursor solution $Fe^{3+}$ ions reduced Fe metal and deposited on the surface of the $TiO_2$ layer.

The XRD characterization aims to determine the structure and crystal size of $TiO_2$ coated on ITO glass before and after Fe metal electrodeposition. The crystal structure and size of $TiO_2$ significantly affect the efficiency of the resulting DSSC because it affects the surface area of dye absorption. The characterization results using XRD are in the form of a diffraction pattern (diffractogram) consisting of peaks characterization of $TiO_2$, as shown in **Figure 6** with the interpretation of the data in **Tables 1** and **2**.

Based on **Figure 6**, there were characteristic peaks of $TiO_2$. The peak with the highest intensity of $TiO_2$ was at 25.33. The data interpretation card d(Å) for crystals was close to 3.5154, 2.3732, and 1.8935. The d(Å) peaks of $TiO_2$ were close to the interpretation card of 3.5157 (**Table 1**).

**Tabel 1**. $TiO_2$ layer interpretation

| 2θ | d(Å) | $I/I_0$ | B | D (nm) |
|---|---|---|---|---|
| 25.33 | 3.5157 | 1000.00 | 0.0023 | 61.8439 |
| 37.83 | 2.3783 | 121.59 | 0.0023 | 63.7834 |
| 48.06 | 1.8931 | 140.44 | 0.0023 | 66.0648 |
| 48.21 | 1.8877 | 106.93 | 0.0023 | 66.1034 |
| 54.07 | 1.6960 | 71.50 | 0.0017 | 91.6499 |

**Tabel 2**. $TiO_2$-Fe layer interpretation

| 2θ | d(Å) | $I/I_0$ | B | D (nm) |
|---|---|---|---|---|
| 25.23 | 3.5266 | 1000.00 | 0.0023 | 61.8317 |
| 37.73 | 2.3821 | 140.27 | 0.0035 | 41.9023 |
| 47.97 | 1.8950 | 148.28 | 0.0017 | 89.3500 |
| 53.82 | 1.7017 | 83.43 | 0.0023 | 67.6661 |
| 55.00 | 1.6683 | 85.53 | 0.0023 | 68.0252 |

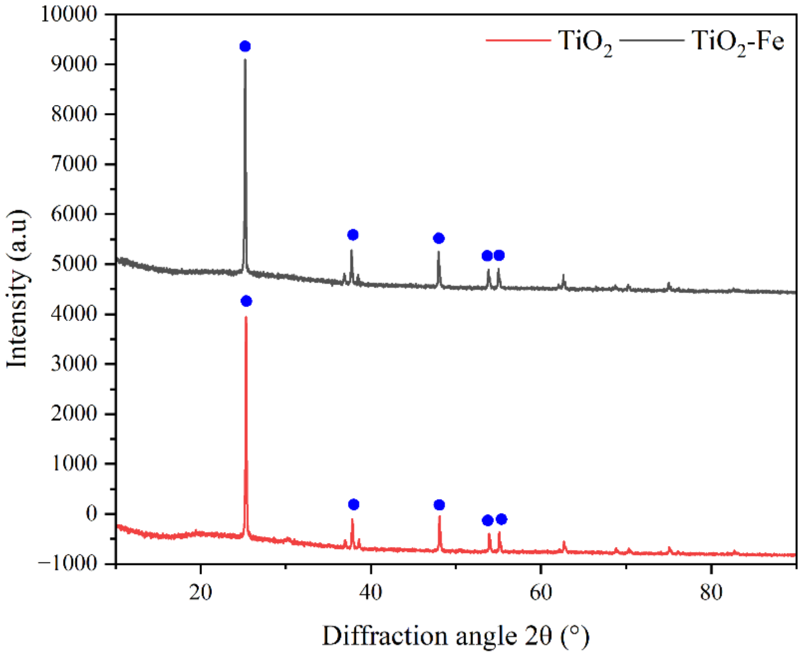


**Figure 6**. Difratogram of XRD analysis for $TiO_2$ before and after electrodeposition

The crystal size of $TiO_2$ affects the surface area, which affects the efficiency of the cell. The crystal size of the XRD data can be calculated using the Scherrer equation.

$$D = \frac{K\lambda}{\beta cos\theta} \quad (1)$$

Where D is the crystallite size in nanometers (nm), K is the Scherrer constant, λ = 1.5406 Å. The parameter β indicates the full width at half maximum (FWHM) of the diffraction peak in radians, while θ is the diffraction angle (Bragg angle) in degrees. This equation is used to determine the crystallite size based on the broadening of the diffraction peaks in the XRD pattern, which provides important information about the crystallinity of the material.

The calculated crystal size of $TiO_2$ was 61.8439 nanometers. The nanometer-sized titanium dioxide crystals enhance the performance of the DSSC. Titanium dioxide is a crystal with a tetragonal structure and anatase phase. The small size of $TiO_2$ crystals with the anatase phase causes the surface area to increase so that the absorption of anthocyanins will be higher, and the performance of solar cells will increase.

The $TiO_2$ layer deposited with the highest intensity Fe metal was found at 2θ = 25.23, with a d(Å) value of 3.5266. From the calculation result, the crystal size of $TiO_2$ was 61.8317 nm. When compared with the size of the crystal before the deposition of Fe metal, there was no significant change in the crystal size. It was possible because Fe metal only forms metal contacts with $TiO_2$.

The crystal size of $TiO_2$ influences the surface area, which in turn affects the efficiency of the DSSC. As shown in our XRD results, the $TiO_2$ crystal size is approximately 61.84–91.65 nm. Smaller crystal sizes provide a larger surface area for dye adsorption, enhancing light absorption and electron injection. This improves charge separation and reduces electron recombination, leading to better DSSC efficiency. Our findings, as shown in **Table 3**, confirm that smaller $TiO_2$ crystals contribute to higher photocurrent and overall efficiency.

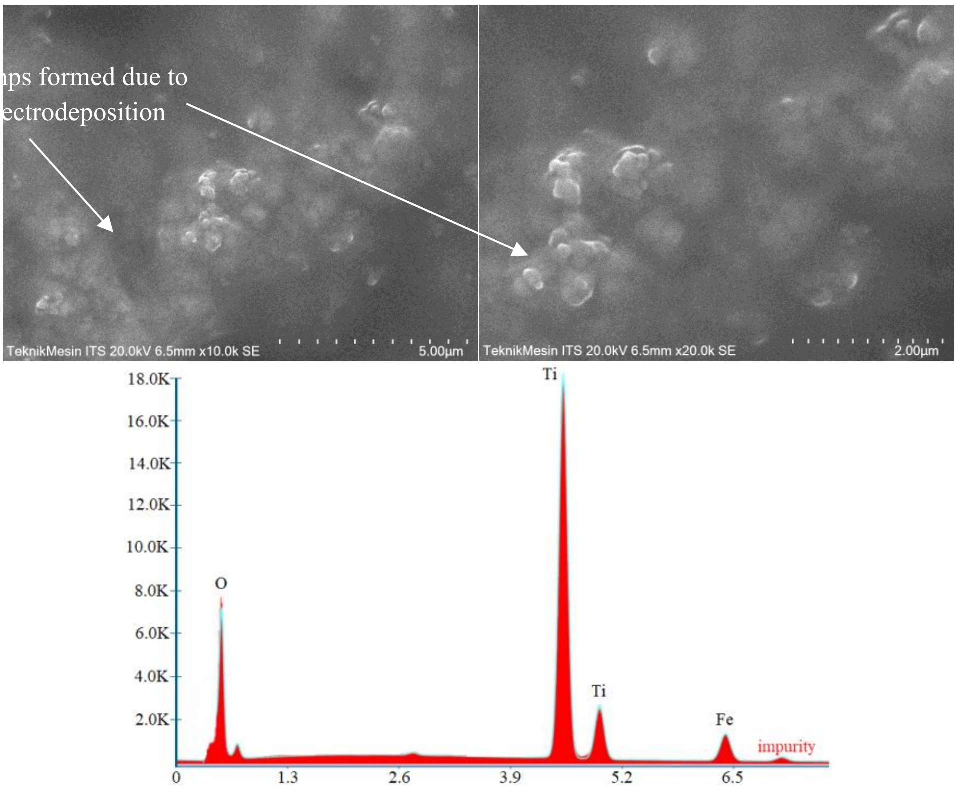


| Element | O K | Ti K | Fe K |
|---|---|---|---|
| Weight % | 45.060 | 48.14 | 6.80 |
| Atomic % | 71.420 | 25.49 | 3.09 |
| Net Int. | 480.610 | 2296.87 | 185.94 |
| Error % | 10.280 | 1.53 | 3.49 |
| Kratio | 0.059 | 0.43 | 0.05 |
| Z | 1.125 | 0.88 | 0.87 |
| A | 0.116 | 1.00 | 0.94 |
| F | 1.000 | 1.00 | 1.01 |

**Figure 7.** SEM-EDS Test Results

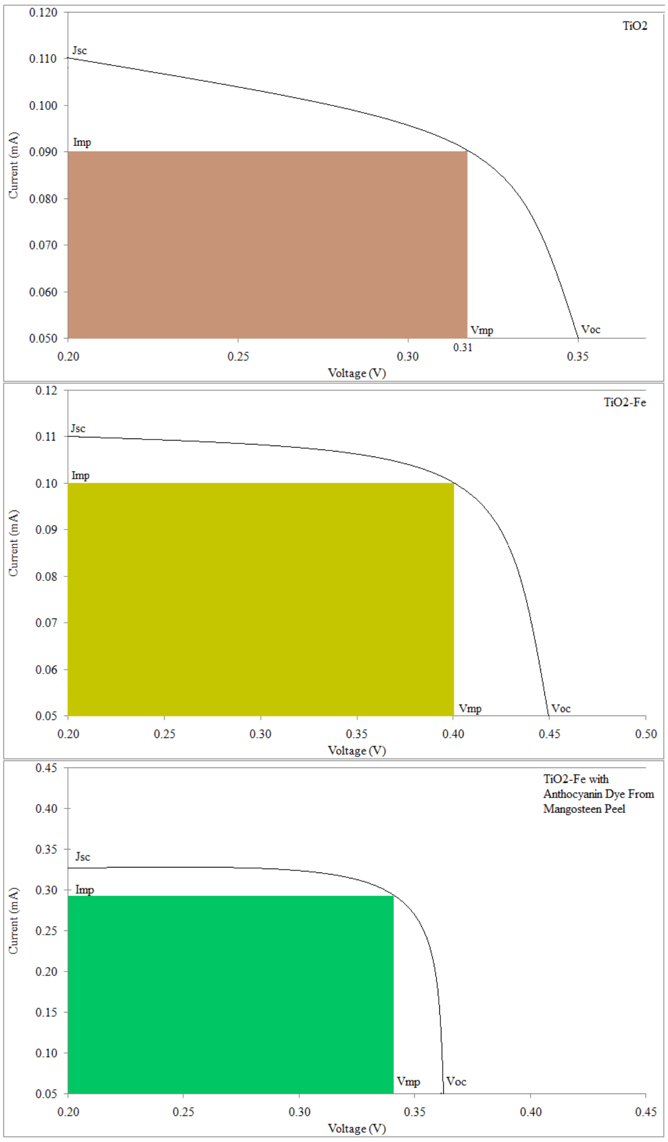


**Figure 8**. I-V characteristic curves for $TiO_2$ electrodes with and without Fe deposition and when the dye is added.

**Table 3**. DSSC efficiency of Fe electrodeposition on $TiO_2$ and dye extracts from natural ingredients.

| | Voc | Isc (mA) | Jsc | FF | efisiensi |
|---|---|---|---|---|---|
| $TiO_2$ | 0.35 | 2.17 | 0.11 | 0.76 | 1.189 |
| $TiO_2$-Fe | 0.45 | 1.84 | 0.11 | 0.83 | 1.700 |
| *Jengkol* peel | 0.35 | 2.40 | 0.16 | 0.84 | 1.925 |
| Grape peel | 0.5 | 1.62 | 0.15 | 0.81 | 2.569 |
| *Senduduk* fruit | 0.48 | 1.75 | 0.21 | 0.84 | 3.495 |
| Mangosteen Peel | 0.36 | 2.39 | 0.32 | 0.86 | 4.123 |

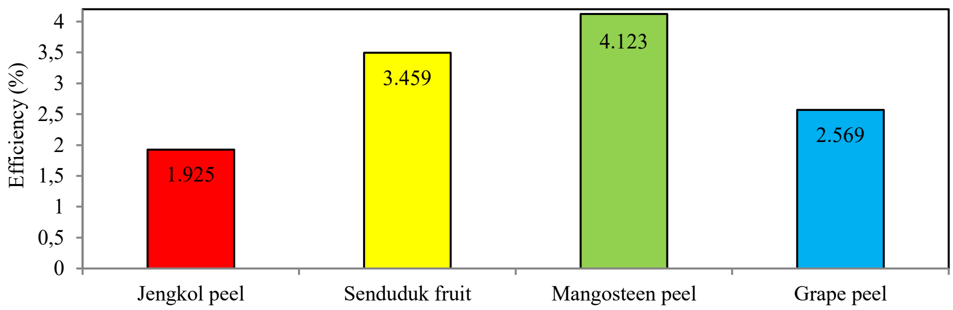


**Figure 9**. Curve comparison of various anthocyanin sources on the efficiency of DSSC

SEM-EDS analysis was performed to understand the surface structure of the $TiO_2$-Fe layer, especially how Fe is dispersed on it. The observations show that Fe forms small clumps that are evenly distributed over the $TiO_2$ layer. These Fe clumps play an important role as metal contacts that prevent the electrons in the dye from recombining with the electrolyte, while accelerating the flow of electrons towards the ITO glass which has high conductivity. The presence of Fe in this layer was confirmed through EDS analysis, which revealed the composition of the materials in the sample. The results show that the coating consists of 45.06% Oxygen (O), 48.14% Titanium (Ti), and 6.8% Iron (Fe). This analysis provides a better understanding of the structure and composition of the $TiO_2$-Fe layer, which plays an important role in improving solar cell performance.

**Efficiency Measurement**

Performance measurements of Substance-Sensitized Solar Cells (DSSCs) are carried out using careful methods to ensure accurate results. Researchers used a 24-watt UV lamp as a stable light source, replacing direct sunlight whose intensity can fluctuate. A multimeter was used to measure voltage and current, while a 100K potentiometer was used to measure electrical power. The efficiency of the solar cell was determined by calculating the maximum power point (MPP) from the I-V curve and fill factor (FF).

The values of Voc, Isc, Jsc, FF, and efficiency in **Table 3** were obtained from the I-V curves shown in **Figure 8**. These values were extracted using **Equations** (**1**)–(**3**), where Voc is determined as the x-intercept of the curve, and Isc as the y-intercept. The fill factor (FF) and efficiency were calculated based on the maximum power point (Vmp, Imp) derived from the I-V characteristics. To enhance clarity, we have labeled key parameters in **Figure 8**, highlighting Voc and Isc values for each condition.

The results showed an increase in DSSC efficiency from 1.189% without Fe coating to 1.700% with the addition of Fe coating. This Fe layer plays a role in reducing electron recombination, thus increasing the efficiency of solar cells. In addition, the smaller $TiO_2$ crystal size also contributes to the increase in efficiency as it provides a larger surface area to absorb the dye.

Although there is an improvement, this increase in efficiency is not very significant. Further analysis revealed that the amount of Fe attached to the $TiO_2$ surface was very small and uneven, forming incoherent clumps. This results in less than optimal protection against electron recombination. In conclusion, the addition of the Fe layer did increase the efficiency of the DSSC, but there is still room for improvement in the manufacturing process to achieve more optimal results. The electrical properties of the DSSC were also measured after the addition of anthocyanin dyes from various natural sources. The results obtained are shown in **Figure 9**.

This study revealed that the combination of $TiO_2$-Fe with various dye copigments produced DSSCs with diverse performance. The DSSC efficiencies of the different dye sources showed significant variations, with *jengkol* skin producing the lowest efficiency of 1.925%, followed by grape skin (2.569%), *senduduk* fruit (3.495%), and mangosteen skin achieving the highest efficiency of 4.123%. The superiority of mangosteen peel can be explained by several key factors. First, copigmentation with salicylic acid increases the absorbance and absorbance intensity of the dye. Second, the maximum wavelength of mangosteen peel at 515 nm indicates that the anthocyanin-salicylic acid complex requires relatively low energy to excite electrons. This process begins when electrons are excited from the conduction band to the valence band in the mangosteen peel extract, then flow to $TiO_2$. This low excitation energy allows for more efficient electron transfer from the dye to the $TiO_2$ and the outer circuit of the DSSC, ultimately improving the overall performance of the solar cell. These results demonstrate the significant potential of mangosteen peel as an effective natural dye source for DSSC applications, especially when combined with copigmentation techniques using salicylic acid.

## CONCLUSIONS

This study demonstrates the potential of Fe electrodeposition on $TiO_2$ combined with pigmented natural dyes to enhance the efficiency of dye-sensitized solar cells (DSSCs). The copigmentation of anthocyanins with salicylic acid was found to improve thermal stability by forming hydrogen bonds and metal complexes that reduce degradation. Furthermore, this copigmentation induces a bathochromic effect, shifting the absorption towards longer wavelengths due to changes in the electronic environment of anthocyanins.

Electrodeposition of Fe on the $TiO_2$ layer reduces electron recombination, enhancing DSSC efficiency. The combination of $TiO_2$-Fe layers with pigmented dyes resulted in varied DSSC performances, with mangosteen peel showing the highest efficiency (4.123%), followed by senduduk fruit (3.495%), grape peel (2.569%), and jengkol peel (1.925%). The superior performance of mangosteen peel is attributed to its high anthocyanin content, particularly cyanidin and delphinidin, which have extensive conjugation and strong light absorption in the DSSC wavelength range.

The increase in efficiency from 1.189% (without Fe coating) to 1.700% (with Fe coating) highlights the potential of this approach. Additionally, the small $TiO_2$ crystal size (61.8 nm) enhances the surface area, improving dye adsorption and solar cell performance. These findings suggest that Fe electrodeposition on $TiO_2$, combined with anthocyanin-rich natural dyes (particularly from mangosteen peel), presents a promising strategy for developing more efficient and sustainable DSSCs.

## REFERENCES

Abdullah, H., Khan, Md. M. R., Ong, H. R., & Yaakob, Z. (2017). Modified $TiO_2$ photocatalyst for $CO_2$ photocatalytic reduction: An overview. *Journal of $CO_2$ Utilization, 22*, 15–32. https://doi.org/10.1016/j.jcou.2017.08.004

Ahmed, M., Huan, W., Ali, N., Shafi, A., Ehsan, M., Abdelrahman, K., & Fnais, M. S. (2023). The effect of energy consumption, income, and population growth on $CO_2$ emissions: Evidence from NARDL and machine learning models. *Sustainability, 15*(15), 11956. https://doi.org/10.3390/su151511956

Arjmand, F., Rashidi Ranjbar, Z., & Fatemi, E. G. H. (2022). Effect of dye complex structure on performance in DSSCs: An experimental and theoretical study. *Heliyon, 8*(11), e11692. https://doi.org/10.1016/j.heliyon.2022.e11692

Augustowski, D., Gala, M., Kwaśnicki, P., & Rysz, J. (2021). Efficiency boost in dye-sensitized solar cells by post-annealing UV-ozone treatment of $TiO_2$ mesoporous layer. *Materials, 14*(16), 4698. https://doi.org/10.3390/ma14164698

Badawy, S. A., Abdel-Latif, E., & Elmorsy, M. R. (2024). Tandem dye-sensitized solar cells achieve 12.89% efficiency using novel organic sensitizers. *Scientific Reports, 14*(1), 26072. https://doi.org/10.1038/s41598-024-75959-0

Badawy, S. A., Abdel-Latif, E., Fadda, A. A., & Elmorsy, M. R. (2022). Synthesis of innovative triphenylamine-functionalized organic photosensitizers outperformed the benchmark dye N719 for high-efficiency dye-sensitized solar cells. *Scientific Reports, 12*(1), 12885. https://doi.org/10.1038/s41598-022-17041-1

Barichello, J., Mariani, P., Vesce, L., Spadaro, D., Citro, I., Matteocci, F., & Calogero, G. (2024). Bifacial dye-sensitized solar cells for indoor and outdoor renewable energy-based application. *Journal of Materials Chemistry C, 12*(7), 2317–2349. https://doi.org/10.1039/D3TC03220E

Baruah, M. J., Dutta, R., Zaki, M. E. A., & Bania, K. K. (2024). Heterogeneous iron-based catalysts for organic transformation reactions: A brief overview. *Molecules, 29*(13), 3177. https://doi.org/10.3390/molecules29133177

Bella, F., Gerbaldi, C., Barolo, C., & Grätzel, M. (2015). Aqueous dye-sensitized solar cells. *Chemical Society Reviews, 44*(11), 3431–3473. https://doi.org/10.1039/C4CS00456F

Benesperi, I., Michaels, H., & Freitag, M. (2018). The researcher's guide to solid-state dye-sensitized solar cells. *Journal of Materials Chemistry C, 6*(44), 11903–11942. https://doi.org/10.1039/C8TC03542C

Bernabé-Poveda, M.-Á., Gołębiowska, I., Narváez-Benalcázar, R., León-Pazmiño, M.-F., Gonzalez-Campos, M.-E., & Çöltekin, A. (2024). Sunshine around the middle Earth: Relief inversion less prevalent in satellite images in the near-south of the Equator than on the Equator. *International Journal of Digital Earth, 17*(1). https://doi.org/10.1080/17538947.2024.2304078

Bin Abu Sofian, A. D. A., Lim, H. R., Siti Halimatul Munawaroh, H., Ma, Z., Chew, K. W., & Show, P. L. (2024). Machine learning and the renewable energy revolution: Exploring solar and wind energy solutions for a sustainable future including innovations in energy storage. *Sustainable Development, 32*(4), 3953–3978. https://doi.org/10.1002/sd.2885

Bonomo, M., Di Girolamo, D., Piccinni, M., Dowling, D. P., & Dini, D. (2020). Electrochemically deposited NiO films as a blocking layer in p-type dye-sensitized solar cells with an impressive 45% fill factor. *Nanomaterials, 10*(1), 167. https://doi.org/10.3390/nano10010167

Calogero, G., Yum, J.-H., Sinopoli, A., Di Marco, G., Grätzel, M., & Nazeeruddin, M. K. (2012). Anthocyanins and betalains as light-harvesting pigments for dye-sensitized solar cells. *Solar Energy, 86*(5), 1563–1575. https://doi.org/10.1016/j.solener.2012.02.018

Chauke, N. M., Mohlala, R. L., Ngqoloda, S., & Raphulu, M. C. (2024). Harnessing visible light: Enhancing $TiO_2$ photocatalysis with photosensitizers for sustainable and efficient environmental solutions. *Frontiers in Chemical Engineering, 6*. https://doi.org/10.3389/fceng.2024.1356021

Chen, C.-Y., Lin, T.-Y., Chiu, C.-F., Lee, M. M., Li, W.-L., Chen, M.-Y., & Wu, C.-G. (2024). Steric effects on the photovoltaic performance of panchromatic ruthenium sensitizers for dye-sensitized solar cells. *ACS Applied Materials & Interfaces, 16*(10), 12647–12660. https://doi.org/10.1021/acsami.3c19298

Dai, Q., & Rabani, J. (2002). Photosensitization of nanocrystalline $TiO_2$ films by anthocyanin dyes. *Journal of Photochemistry and Photobiology A: Chemistry, 148*(1–3), 17–24. https://doi.org/10.1016/S1010-6030(02)00073-4

D'Amico, F., de Jong, B., Bartolini, M., Franchi, D., Dessì, A., Zani, L., & Vesce, L. (2023). Recent advances in organic dyes for application in dye-sensitized solar cells under indoor lighting conditions. *Materials, 16*(23), 7338. https://doi.org/10.3390/ma16237338

Darmawan, M. I., & Nuzuluddin, M. (2023). Dye-sensitized solar cells (DSSC) use natural organic sulphur cosmos leaves. *Kappa Journal, 7*(2), 289–293. https://doi.org/10.29408/kpj.v7i2.20932

Dragonetti, C., & Colombo, A. (2021). Recent advances in dye-sensitized solar cells. *Molecules, 26*(9), 2461. https://doi.org/10.

3390/molecules26092461

Elmorsy, M. R., Abdelhamed, F. H., Badawy, S. A., Abdel-Latif, E., Abdel-Shafi, A. A., & Ismail, M. A. (2023). Design, synthesis, and performance evaluation of $TiO_2$-dye sensitized solar cells using 2,2′-bithiophene-based co-sensitizers. *Scientific Reports, 13*(1), 13825. https://doi.org/10.1038/s41598-023-40830-1

Emerson, D., Sofen, L. E., Michaud, A. B., Archer, S. D., & Twining, B. S. (2024). A cost model for ocean iron fertilization as a means of carbon dioxide removal that compares ship- and aerial-based delivery, and estimates verification costs. *Earth's Future, 12*(4). https://doi.org/10.1029/2023EF003732

Gatou, M.-A., Syrrakou, A., Lagopati, N., & Pavlatou, E. A. (2024). Photocatalytic $TiO_2$-based nanostructures as a promising material for diverse environmental applications: A review. *Reactions, 5*(1), 135–194. https://doi.org/10.3390/reactions5010007

Gnida, P., Jarka, P., Chulkin, P., Drygała, A., Libera, M., Tański, T., & Schab-Balcerzak, E. (2021). Impact of $TiO_2$ nanostructures on dye-sensitized solar cells performance. *Materials, 14*(7), 1633. https://doi.org/10.3390/ma14071633

Gorina, L., Korneeva, E., Kovaleva, O., & Strielkowski, W. (2024). Energy-saving technologies and energy efficiency in the post-COVID era. *Sustainable Development, 32*(5), 5294–5310. https://doi.org/10.1002/sd.2978

Hardeli, Hijri, F., Sanjaya, H., Putri, Y. P., & Permatasari, P. (2023). The effect of coating in increasing the efficiency of solar cells by using quercetin poly as a dye. *Rasayan Journal of Chemistry, 16*(3), 1925–1931. https://doi.org/10.31788/RJC.2023.1638143

Hardeli, Sanjaya, H., Permatasari, P., Novita, I. P., Agdisti, N. F., Luli, R., & Yunita, L. (2022). $TiO_2$-Ag and natural dye co-pigmented with salicylic acid for dye-sensitized solar cell (DSSC) application. *Rasayan Journal of Chemistry, 15*(1), 569–578. https://doi.org/10.31788/RJC.2022.1516567

Hsu, C.-Y., Al-Salman, H. N. K., Mahmoud, Z. H., Ahmed, R. M., & Dawood, A. F. (2024). Improvement of the photoelectric dye-sensitized solar cell performance using Fe/S–$TiO_2$ nanoparticles as photoanode electrode. *Scientific Reports, 14*(1), 4931. https://doi.org/10.1038/s41598-024-54895-z

Jiglau, G., Hesselman, M., Dobbins, A., Grossmann, K., Guyet, R., Tirado Herrero, S., & Varo, A. (2024). Energy and the social contract: From "energy consumers" to "people with a right to energy." *Sustainable Development, 32*(1), 1321–1336. https://doi.org/10.1002/sd.2727

Kusuma, H. H. (2017). The characteristics of material DSSC (dye-sensitized solar cell) solar cell from extraction of teak leaves. *Journal of Natural Sciences and Mathematics Research, 2*(1), 117–121. https://doi.org/10.21580/jnsmr.2016.1.1.1645

LaBelle, M. C. (2023). Energy as a weapon of war: Lessons from 50 years of energy interdependence. *Global Policy, 14*(3), 531–547. https://doi.org/10.1111/1758-5899.13235

Lee, Y.-J., Kim, B.-S., Ifitiquar, S. M., Park, C., & Yi, J. (2014). Silicon solar cells: Past, present and the future. *Journal of the Korean Physical Society, 65*(3), 355–361. https://doi.org/10.3938/jkps.65.355

Leela Devi, V., De, D., Kuchhal, P., & Pachauri, R. K. (2024). Photovoltaic performance of $TiO_2$ and ZnO nanostructures in anthocyanin dye-sensitized solar cells. *Clean Energy, 8*(5), 144–156. https://doi.org/10.1093/ce/zkae059

Leijtens, T., Eperon, G. E., Barker, A. J., Grancini, G., Zhang, W., Ball, J. M., … Petrozza, A. (2016). Carrier trapping and recombination: The role of defect physics in enhancing the open circuit voltage of metal halide perovskite solar cells. *Energy & Environmental Science, 9*(11), 3472–3481. https://doi.org/10.1039/C6EE01729K

Li, N., Wang, Q., Zhou, J., Li, S., Liu, J., & Chen, H. (2022). Insight into the progress on natural dyes: Sources, structural features, health effects, challenges, and potential. *Molecules, 27*(10), 3291. https://doi.org/10.3390/molecules27103291

Li, R., Li, T., & Zhou, Q. (2020). Impact of titanium dioxide ($TiO_2$) modification on its application to pollution treatment—A review. *Catalysts, 10*(7), 804. https://doi.org/10.3390/catal10070804

Longo, C., & De Paoli, M.-A. (2003). Dye-sensitized solar cells: A successful combination of materials. *Journal of the Brazilian Chemical Society, 14*(6). https://doi.org/10.1590/S0103-50532003000600005

Mariotti, N., Bonomo, M., Fagiolari, L., Barbero, N., Gerbaldi, C., Bella, F., & Barolo, C. (2020). Recent advances in eco-friendly and cost-effective materials towards sustainable dye-sensitized solar cells. *Green Chemistry, 22*(21), 7168–7218. https://doi.org/10.1039/D0GC01148G

Mauri, L., Colombo, A., Dragonetti, C., & Fagnani, F. (2022). A fascinating trip into iron and copper dyes for DSSCs. *Inorganics, 10*(9), 137. https://doi.org/10.3390/inorganics10090137

Maurya, I. C., Neetu, Gupta, A. K., Srivastava, P., & Bahadur, L. (2016). Natural dye extracted from *Saraca asoca* flowers as sensitizer for $TiO_2$-based dye-sensitized solar cell. *Journal of Solar Energy Engineering, 138*(5), 051006. https://doi.org/10.1115/1.4034028

Mombekova, G., Nurgabylov, M., Baimbetova, A., Keneshbayev, B., & Izatullayeva, B. (2024). The relationship between energy consumption, population, and economic growth in developing countries. *International Journal of Energy Economics and Policy, 14*(3), 368–374. https://doi.org/10.32479/ijeep.15614

Muhammad Rizki Azra, Tamrin, & Haisen Hower. (2024). Analysis performance of dye-sensitized solar cells (DSSC) of single and double mixed natural dye as photosensitizers. *World Journal of Advanced Research and Reviews, 23*(3), 2324–2328. https://doi.org/10.30574/wjarr.2024.23.3.2892

Mulijani, S., Syahbirin, G., Wulanawati, A., Marita, B., Saputra, A., Shabrina, & Nurbakti, M. (2020). Enhancement of efficiency of natural dye on harvesting solar energy by incorporated montmorillonite nanoparticle. *Rasayan Journal of Chemistry, 13*(3), 1612–1618. https://doi.org/10.31788/RJC.2020.1335649

Muñoz-García, A. B., Benesperi, I., Boschloo, G., Concepcion, J. J., Delcamp, J. H., Gibson, E. A., … Freitag, M. (2021). Dye-sensitized solar cells strike back. *Chemical Society Reviews, 50*(22), 12450–12550. https://doi.org/10.1039/D0CS01336F

Mustafa, F. M., Abdel Khalek, A. A., Mahboob, A. A., & Abdel-Latif, M. K. (2023). Designing efficient metal-free dye-sensitized solar cells: A detailed computational study. *Molecules, 28*(17), 6177. https://doi.org/10.3390/molecules28176177

Nijsse, F. J. M. M., Mercure, J.-F., Ameli, N., Larosa, F., Kothari, S., Rickman, J., … Pollitt, H. (2023). The momentum of the solar energy transition. *Nature Communications, 14*(1), 6542. https://doi.org/10.1038/s41467-023-41971-7

Novita, N., Abd. Madjid, S., Bahi, M., Irvanizam, I., Erni, E., & Angraini, I. (2024). Utilisation of natural dyes from Nipah fruit skin (*Nypa fruticans*) using the Shibori technique in fashion products. *International Journal of Applied Science and Engineering Review, 5*(3), 76–84. https://doi.org/10.52267/IJASER.2024.5310

Nyamukamba, P., Okoh, O., Mungondori, H., Taziwa, R., & Zinya, S. (2018). Synthetic methods for titanium dioxide nanoparticles: A review. In *Titanium Dioxide - Material for a Sustainable Environment*. InTech. https://doi.org/10.5772/intechopen.75425

Pambudi, N. A., Firdaus, R. A., Rizkiana, R., Ulfa, D. K., Salsabila, M. S., Suharno, & Sukatiman. (2023). Renewable energy in Indonesia: Current status, potential, and future development. *Sustainability, 15*(3), 2342. https://doi.org/10.3390/su15032342

Pashiri, N. T., Ameli, M. T., & Azad, S. (2022). An overview of the transition from one-dimensional energy networks to multi-carrier energy grids. In *Coordinated Operation and Planning of Modern Heat and Electricity Incorporated Networks* (pp. 13–29). Wiley. https://doi.org/10.1002/9781119862161.ch2

Pollin, R. (2023). The political economy of saving the planet. *The Japanese Political Economy, 49*(2–3), 141–168. https://doi.org/10.1080/2329194X.2023.2262531

Prabavathy, N., Shalini, S., Balasundaraprabhu, R., Velauthapillai, D., Prasanna, S., Walke, P., & Muthukumarasamy, N. (2017). Effect of solvents in the extraction and stability of anthocyanin from the petals of *Caesalpinia pulcherrima* for natural dye-sensitized solar cell applications. *Journal of Materials Science: Materials in Electronics, 28*(13), 9882–9892. https://doi.org/10.1007/s10854-017-6743-7

Racovita, A. D. (2022). Titanium dioxide: Structure, impact, and toxicity. *International Journal of Environmental Research and Public Health, 19*(9), 5681. https://doi.org/10.3390/ijerph19095681

Rahman, S., Haleem, A., Siddiq, M., Hussain, M. K., Qamar, S., Hameed, S., & Waris, M. (2023). Research on dye-sensitized solar cells: Recent advancement toward the various constituents of dye-sensitized solar cells for efficiency enhancement and future prospects. *RSC Advances, 13*(28), 19508–19529. https://doi.org/10.1039/D3RA00903C

Rodríguez-Rojas, M. del P., Bustos-Terrones, V., Díaz-Cárdenas, M. Y., Vázquez-Vélez, E., & Martínez, H. (2024). Life cycle assessment of green synthesis of $TiO_2$ nanoparticles vs. chemical synthesis. *Sustainability, 16*(17), 7751. https://doi.org/10.3390/su16177751

Sahin, H., Solomon, A. A., Aghahosseini, A., & Breyer, C. (2024). Systemwide energy return on investment in a sustainable transition towards net zero power systems. *Nature Communications, 15*(1), 208. https://doi.org/10.1038/s41467-023-44232-9

Salauddin Sk, Md., Mia, R., Haque, Md. A., & Shamim, A. M. (2021). Review on extraction and application of natural dyes. *Textile & Leather Review.* https://doi.org/10.31881/TLR.2021.09

Setyawati, H., Darmokoesoemo, H., Ningtyas, A. T. A., Kadmi, Y., Elmsellem, H., & Kusuma, H. S. (2017). Effect of metal ion Fe(III) on the performance of chlorophyll as photosensitizers on dye-sensitized solar cells. *Results in Physics, 7*, 2907–2918. https://doi.org/10.1016/j.rinp.2017.08.009

Sharma, K., Sharma, V., & Sharma, S. S. (2018a). Dye-sensitized solar cells: Fundamentals and current status. *Nanoscale Research Letters, 13*(1), 381. https://doi.org/10.1186/s11671-018-2760-6

Sharma, K., Sharma, V., & Sharma, S. S. (2018b).

Dye-sensitized solar cells: Fundamentals and current status. *Nanoscale Research Letters, 13*(1), 381. https://doi.org/10.1186/s11671-018-2760-6

Sherkar, T. S., Momblona, C., Gil-Escrig, L., Ávila, J., Sessolo, M., Bolink, H. J., & Koster, L. J. A. (2017). Recombination in perovskite solar cells: Significance of grain boundaries, interface traps, and defect ions. *ACS Energy Letters, 2*(5), 1214–1222. https://doi.org/10.1021/acsenergylett.7b00236

Silalahi, D. F., Blakers, A., Stocks, M., Lu, B., Cheng, C., & Hayes, L. (2021). Indonesia's vast solar energy potential. *Energies, 14*(17), 5424. https://doi.org/10.3390/en14175424

Subramanian, A., & Wang, H.-W. (2012). Effect of hydroxyl group attachment on $TiO_2$ films for dye-sensitized solar cells. *Applied Surface Science, 258*(20), 7833–7838. https://doi.org/10.1016/j.apsusc.2012.04.069

Thu, D. X., Trung, V. Q., Nghia, N. M., Khang, N. C., & Lam, T. D. (2016). Effects of Fe doping on the structural, optical, and magnetic properties of $TiO_2$ nanoparticles. *Journal of Electronic Materials, 45*(11), 6033–6037. https://doi.org/10.1007/s11664-016-4825-6

Triyanto, A., Ali, N., Salleh, H., Setiawan, J., & Yatim, N. I. (2024). Development of natural dye photosensitizers for dye-sensitized solar cells: A review. *Environmental Science and Pollution Research, 31*(22), 31679–31690. https://doi.org/10.1007/s11356-024-33360-4

Tuharin, K., Turek, Z., Zanáška, M., Kudrna, P., & Tichý, M. (2020). Iron oxide and iron sulfide films prepared for dye-sensitized solar cells. *Materials, 13*(8), 1797. https://doi.org/10.3390/ma13081797

Wang, C., Song, J., Shi, D., Reyna, J. L., Horsey, H., Feron, S., Zhou, Y., Ouyang, Z., Li, Y. & Jackson, R. B. (2023). Impacts of climate change, population growth, and power sector decarbonization on urban building energy use. *Nature Communications, 14*(1), 6434. https://doi.org/10.1038/s41467-023-41458-5

Widiatmoko, P., Devianto, H., Marcos, J. N., & Ibrahim, Z. R. A. (2024). Dye-sensitized solar cell performance analysis through equivalent circuit model. *AIP Conference Proceedings, 2786*, 020002. https://doi.org/10.1063/5.0195369

Wuryanti, S., & Megawati. (2019). Fin flat-plate type tetragon solar collector design based on convection radiation mechanism. *Cogent Engineering, 6*(1), 1637165. https://doi.org/10.1080/23311916.2019.1637165

Zdyb, A., & Krawczak, E. (2021). Organic dyes in dye-sensitized solar cells featuring back reflector. *Energies, 14*(17), 5529. https://doi.org/10.3390/en14175529

Zhu, Y., Chen, H., Lou, L., Chen, Y., Ye, X., & Chen, J. (2020). Copigmentation effect of three phenolic acids on color and thermal stability of Chinese bayberry anthocyanins. *Food Science & Nutrition, 8*(7), 3234–3242. https://doi.org/10.1002/fsn3.1583